JOURNAL OF MATERIALS SCIENCE **39** (2004) 3683–3688

Influence of calcination temperature on structural and optical properties of TiO_2-SiO_2 thin films prepared by sol-gel dip coating

HAK JOON LEE, SUNG HONG HAHN
Department of Physics, University of Ulsan, Ulsan 680-749, South Korea
E-mail: shhahn@mail.ulsan.ac.kr

EUI JUNG KIM
Department of Chemical Engineering, University of Ulsan, Ulsan 680-749, South Korea

YONG ZOO YOU
School of Materials Science and Engineering, ReMM, Ulsan 680-749, South Korea

We prepared TiO_2-SiO_2 thin films with various TiO_2/SiO_2 ratios by sol-gel dip coating method and explored the dependence of their structural and optical properties on calcination temperature. The absorption peaks relevant to Si–O, Si–O–Ti and Ti–O bonds appeared in the FTIR spectra. With increasing TiO_2 content, the intensity of Si–O bond peaks decreases and that of Ti–O bond peaks increases. The XRD results show that the temperature of transformation from amorphous to anatase phase is lowered as TiO_2 content increases. The crystallite size of anatase phase in composite thin films increases with increasing TiO_2 content and calcination temperature. At 1000°C, the mixed phase of anatase and rutile appears in the pure TiO_2 thin films. The rutile films are denser than the anatase films. The increase in refractive index of composite thin films with calcination temperature is related to the decreased thickness and increased density as a result of evaporation of water and organic matters below 400°C. On the other hand, it is related to the change in the crystal phase and crystallite size of the films over 400°C. © *2004 Kluwer Academic Publishers*

1. Introduction

Sol-gel method is one of the most useful technologies to produce amorphous or crystalline oxide coating [1]. Sol-gel processing enables us to easily control composition and optical properties of the final materials [2, 3]. The control of refractive index and thickness of the thin films is crucial in producing suitable materials for optical applications. The refractive index of TiO_2 films is very different from that of SiO_2 films. Accordingly, a wide range of intermediate index values can be obtained by mixing these materials [4]. TiO_2 and TiO_2-SiO_2 films have been widely investigated for various optical applications [5–10]. Mennig *et al*. [11] and Brinker *et al*. [12] used the sol-gel process to form TiO_2-SiO_2 films having a low refractive index. Jiwei *et al*. [9] and Yanagi *et al*. [13] studied TiO_2-SiO_2 films for use as a waveguide. McCulloch *et al*. [14] reported on the characterization of TiO_2-SiO_2 films intended for use in optical chemical sensor.

The mixing of TiO_2 and SiO_2 in thin films can transform amorphous phase into crystalline anatase, and also anatase into rutile. Thin films of pure TiO_2 generally crystallize in the anatase phase at low temperatures below 600°C and in the rutile phase at high temperatures above 600°C [15]. The addition of small amounts of a glass forming solute (i.e., SiO_2) into TiO_2 films retards crystallization [14]. The structure of the composite films is amorphous for a SiO_2 content of as low as 11 mol% [16]. A good understanding of the process of crystal transformation is necessary for preparing excellent optical films into visible and near-infrared wavelength ranges. The control of the crystal structure for use in optical TiO_2-SiO_2 films is required to tailor their optical properties.

In this paper, we synthesized TiO_2-SiO_2 coating solutions with various TiO_2/SiO_2 ratios and prepared TiO_2-SiO_2 thin films by sol-gel dip coating method. By using Fourier Transform Infrared (FTIR) spectrometry, X-ray Diffraction (XRD), Scanning Electron Microscopy (SEM) and Ultraviolet-Visible (UV/VIS) spectrophotometry techniques, we investigated the influence of TiO_2 content and calcination temperature on optical and structural properties of TiO_2-SiO_2 thin films.

2. Experiments

TiO_2-SiO_2 solutions were prepared by the procedure described as follows. Titanium tetra-isopropoxide (TTIP, $Ti[OCH(CH_3)_2]_4$, 98.0%, Junsei Chemical Inc.) was used as a Ti source material, tetraethyl orthosilicate

(TEOS, $Si[OC_2H_5]_4$, 98.0, Acros Organics) as a Si source material, 0.7N-hydrochloric acid (HCl, 35.0%, Oriental Chemical Industries) as a catalyst, and isopropyl alcohol (Pr^iOH, $[CH_3]_2CHOH$, 99.5, Oriental Chemical Industries) as a solvent. Its typical composition was a molar ratio of TTIP + TEOS:Pr^iOH:0.7N-HCl = 1:26.05:1.4. The sol was under continuous stirring in nitrogen atmosphere at room temperature. The TiO_2 and SiO_2 sols were mixed to get a desired TTIP/TEOS molar ratio of 100/0, 75/25, 50/50 and 25/75, respectively.

The powders were prepared by evaporating solvents from the mixed solutions [17]. A thermal behavior of the powder synthesized was examined by thermogravimetry (TG) and differential scanning calorimetry (DSC) using a Rhometric STA1500 TG/DSC thermal analyzer.

TiO_2-SiO_2 composite thin films were deposited on substrates such as quartz glass (50 × 20 mm) and Si-wafer by sol-gel dip coating at a withdrawal speed of 100 mm/min. The substrate was cleaned with solvent and rinsed with distilled water and then blown with nitrogen gas prior to film deposition. The thickness of as-deposited film was about 350 nm, which was obtained by repeating three times the cycle of dipping in sol followed by drying at 100°C for 30 min in a vacuum oven. This was then subjected to slow heating at a rate of 5°C/min to a desired temperature up to 1000°C and then holding at that temperature for 1 h in a furnace. The furnace was allowed to cool naturally after calcination.

The chemical structure of the thin films was examined using an FTIR spectrophotometer (ATI Matton Genesis Series). For crystal phase identification, XRD patterns were obtained with a diffractometer (Philips PW3710) using Cu K_α radiation at 35 kV and 20 mA. The nano-particle size and morphology were analyzed by a field emission scanning electron microscope (Hitachi S-4200). Optical properties of the films deposited on glass substrates were examined by transmission spectroscopy in the spectral range of 200–1100 nm. The normal incident transmittance of the sample was measured by a UV/VIS spectrophotometer (HP 8453).

3. Results and discussion

3.1. Structural properties

Fig. 1 shows the FTIR spectra of TiO_2-SiO_2 thin films coated on Si-wafer after calcination at 800°C. The absorption peak at about 550 cm^{-1} is characteristic of titanium dioxide [18]. In the FTIR spectra, Si—O bonds appeared near 1100 cm^{-1}, Si—O—Ti bonds near 900 cm^{-1}, and Ti—O bonds near 400 cm^{-1}. The intensity of the peaks near 1100 cm^{-1} decreases with increasing TiO_2 content, while that of the peaks near 400 cm^{-1} increases. The absorption peak at 955 cm^{-1} in the $25TiO_2$-$75SiO_2$ films results from overlapping of the peaks due to Si—OH and Si—O—Ti vibration modes [19]. For the $50TiO_2$-$50SiO_2$ thin films, the Ti—O—Si bond appears at 935 cm^{-1}.

Fig. 2 depicts TG/DSC data for the synthesized $25TiO_2$-$75TiO_2$ powders. For thermal analysis the sample was heated in air at a heating rate of 10°C min^{-1}.

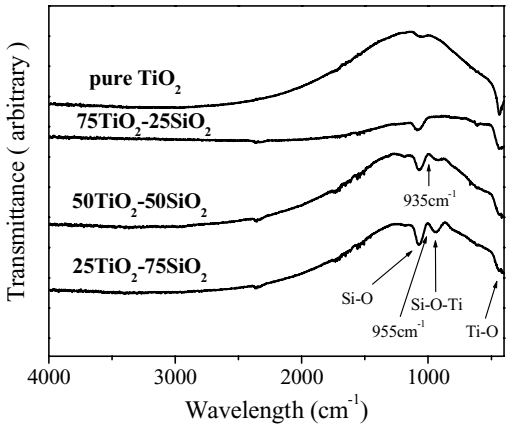

Figure 1 FTIR spectra of TiO_2-SiO_2 thin films calcined at 800°C.

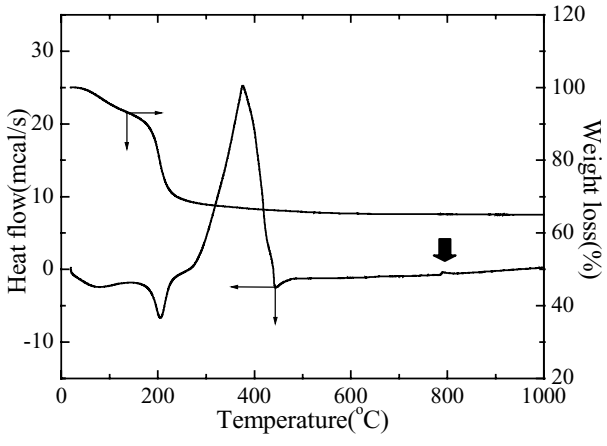

Figure 2 TG/DSC curves of $25TiO_2$-$75SiO_2$ powders synthesized.

The TG curve indicates that the loss of weight took place up to 200°C, and a slight change in weight occurred with further increase in temperature above 200°C. The DSC data show an endothermic peak at 200°C, two exothermic peaks at 380 and 800°C, respectively. The endothermic peak at 200°C is attributed to solvent evaporation. The first exothermic peak at 380°C is due to dehydroxylation and decomposition of residual organics. The other peak at 800°C signifies a phase transition from amorphous phase to crystalline anatase. This peak indicating phase transition from amorphous to anatase in $50TiO_2$-$50TiO_2$, $75TiO_2$-$25TiO_2$ and $100TiO_2$-$0SiO_2$ powders appeared at 600°C, 580°C and 460°C, respectively. The transformation from anatase to rutile was not detected except for $100TiO_2$-$0SiO_2$ powders calcined at 1000°C probably because of the relatively small difference in the enthalpy values between two crystal phases [17].

Fig. 3 illustrates the XRD patterns of the TiO_2-SiO_2 thin films calcined at various temperatures for 1 h. The XRD patterns of the composite thin films show anatase peaks in pure TiO_2 films calcined at 400–800°C, $75TiO_2$-$25SiO_2$ films calcined at 600–1000°C, and $50TiO_2$-$50SiO_2$ films calcined at 800–1000°C. The pure TiO_2 thin films calcined at 1000°C are found to be a mixture of anatase and rutile phases and all calcined $25TiO_2$-$75SiO_2$ thin films are amorphous. The intensity of the XRD peaks of the composite thin films increases with increasing TiO_2 content and calcination

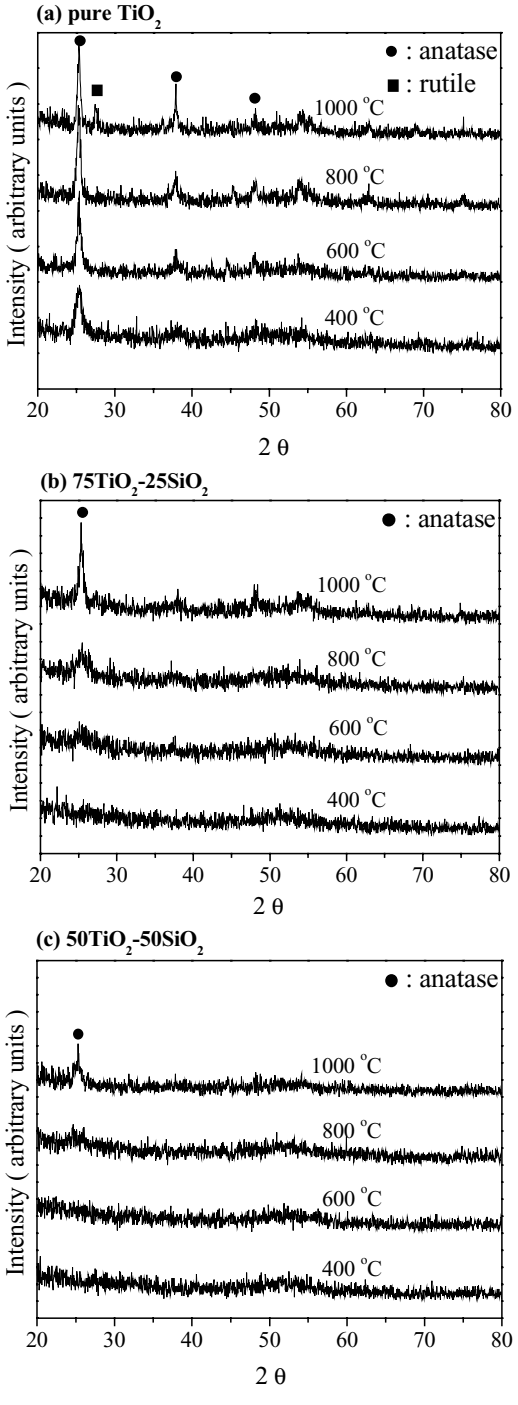

Figure 3 XRD patterns of TiO_2-SiO_2 thin films: (a) pure TiO_2, (b) $75TiO_2$-$25SiO_2$, and (c) $50TiO_2$-$50SiO_2$.

temperature, due to the improvement in crystallinity. The amorphous-to-anatase transformation temperature is lowered with increasing TiO_2 content. These results imply that the formation of the anatase phase is retarded on addition of SiO_2 to the composite thin films.

The crystallite size of composite thin films can be determined from the broadening of corresponding XRD peaks by Scherrer's equation [20]

$$L = \frac{K\lambda}{\beta \cos\theta} \tag{1}$$

where L is the crystallite size of composite thin films, λ is the wavelength of X-ray (Cu $K_\alpha = 1.5406$ Å) radiation, K is usually taken as 0.94 and β is the angle width at half maximum height, and θ is the half diffraction angle of the centroid of the in degree. The peaks of anatase (101) and rutile (110) occurred at $2\theta = 25.3°$ and 27.4°, respectively. Any contributions to broadening due to non-uniform stress were neglected, and the instrumental line-width in the XRD apparatus was subtracted. The calculated crystallite size of the composite thin films is listed in Table I. It is seen that the TiO_2 crystallite size depends on the TiO_2/SiO_2 ratio. The crystallite size of anatase phase in the composite thin films increases with increasing TiO_2 content and calcination temperature. The anatase crystallite size of the composite thin films calcined at 1000°C increases about twice from 11 nm ($50TiO_2$-$50SiO_2$) to 22 nm (pure TiO_2) with increasing TiO_2 content. The crystallite size of pure TiO_2 films is also increased about twice from 11 to 22 nm with increasing calcination temperature from 400 to 1000°C. The rutile crystallite size of the pure TiO_2 thin films calcined at 1000°C is 26 nm, which is larger than the anatase crystallite size. In the TiO_2 film calcined at 1000°C, the weight percentages of anatase and rutile phases are 0.676 and 0.324, respectively [21].

TABLE I Crystallite size of the TiO_2-SiO_2 thin films calcined at various temperatures for 1 h

Calcination temp. (°C)	Composition (mol%)	Crystallite size (nm)	
		Anatase	Rutile
400	Pure TiO_2	11	
	$75TiO_2$-$25SiO_2$	10	
600	Pure TiO_2	20	
	$50TiO_2$-$50SiO_2$	10	
	$75TiO_2$-$25SiO_2$	13	
800	Pure TiO_2	21	
	$50TiO_2$-$50SiO_2$	11	
	$75TiO_2$-$25SiO_2$	20	
1000	Pure TiO_2	22	26

Figs 4 and 5 show the SEM micrographs of the pure TiO_2 and TiO_2-SiO_2 films calcined at various temperatures for 1 h, respectively. The film thickness and film quality of thin films prepared on the substrate are uniform and homogeneous. In Fig. 4a, we can see apparently the crystallinity of the films calcined at 400°C but it is difficult to identify the secondary particles in the films at this temperature. As shown in Fig. 4b, the film calcined at 600°C is composed of the secondary particles of about 20 to 30 nm in size. Here, the primary particles comprising the secondary particles cannot be identified. As the calcination temperature is increased to 800°C, the film becomes in the more agglomerated state whose size is about 40 to 50 nm as a result of densification (Fig. 4c). It is interesting to note in Fig. 4d that the size of secondary particles considerably increases to 150–300 nm at 1000°C and their shape is nonspherical. The $75TiO_2$-$25SiO_2$ films calcined at 600°C (Fig. 5b) and 800°C (Fig. 5c) have anatase phase according to the XRD results, but their SEM images look similar to the amorphous films (Fig. 5a). The film calcined at 1000°C is composed of the highly dense secondary particles of about 30 to 40 nm in size in Fig. 5d. The SEM results show that the rutile films are denser than the

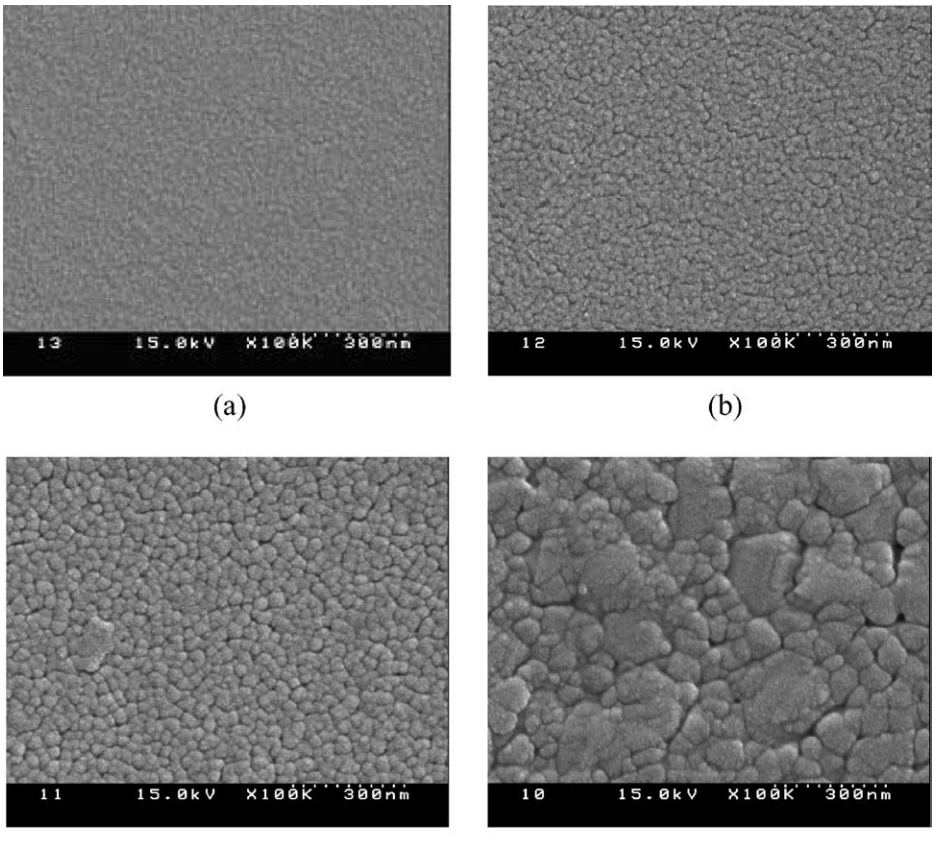

Figure 4 SEM micrographs of pure TiO_2 thin films at various temperatures for 1 h: (a) 400°C, (b) 600°C, (c) 800°C, and (d) 1000°C.

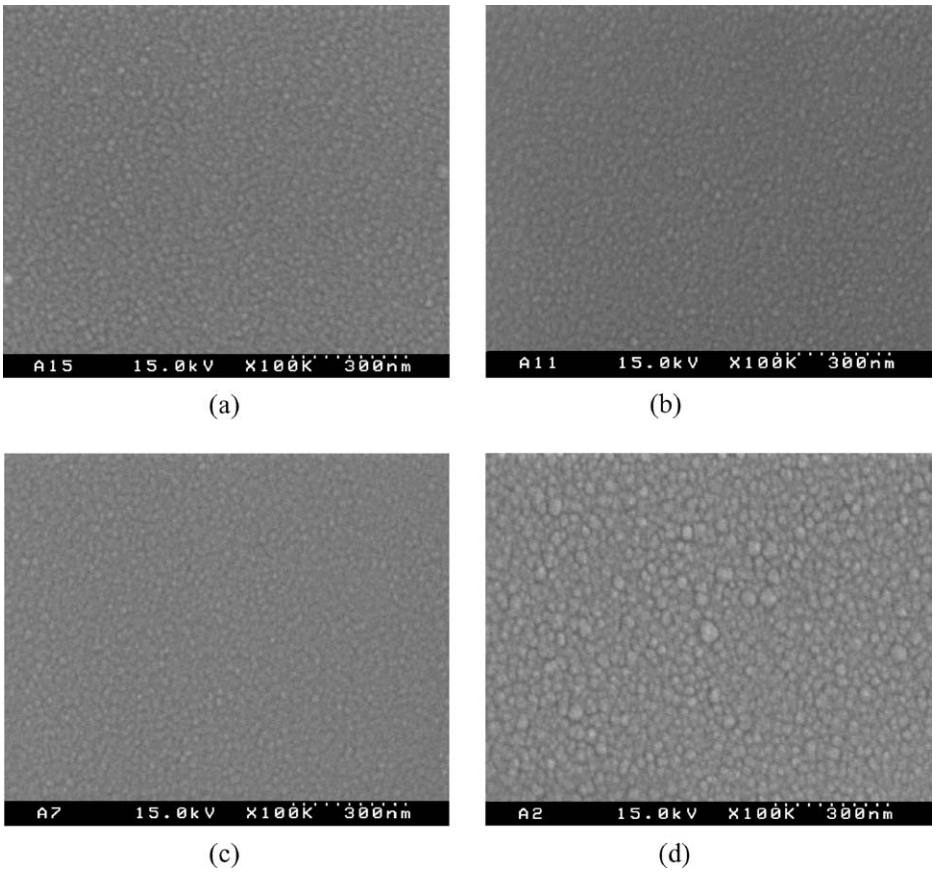

Figure 5 SEM micrographs of $75TiO_2$-$25SiO_2$ thin films at various temperatures for 1 h: (a) 400°C, (b) 600°C, (c) 800°C, and (d) 1000°C.

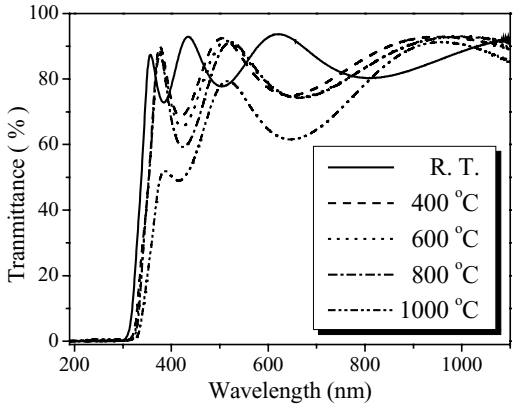

Figure 6 UV-VIS spectra of pure TiO_2 thin films calcined at various temperatures.

anatase films (Figs 4d and 5d). From the above results, the sintering of the nanocrystalline TiO_2-SiO_2 particles is accelerated at higher calcination temperatures and TiO_2/SiO_2 ratios. This is related to a change in the surface structure of films due to crystal phase transformation, which was confirmed by the XRD results [22].

3.2. Optical properties

Fig. 6 shows the transmittance of pure TiO_2 thin films calcined at various temperatures for 1 h. The absorption edge of the rutile thin films calcined at 1000°C is red-shifted in comparison to the anatase thin films calcined at 400–800°C. This shift is ascribed to the difference in band gap energy of the composite thin films resulting from the anatase-to-rutile transformation [23]. A difference in absorption edge between thin films calcined at 400–800°C and as-deposited amorphous film can be explained in a similar way. The transmittance of pure TiO_2 thin films calcined at 1000°C was significantly reduced in the wavelength range of about 300 to 700 nm. This is due to the change in both crystallite phase and film composition and to the scattering effect resulting from the increase in the second grain size. Moreover, the non-stoichiometric film would be formed at higher calcination temperatures. Fig. 7 shows the transmittance of composite thin films calcined at 600°C for 1 h. One can see that the absorption edge of transmittance is red-shifted with increasing TiO_2 content. This is due to the different band gaps of TiO_2 and SiO_2. The optical thickness of the composite thin films increases with increasing TiO_2 content. The maximum peaks of transmittance shifted to a shorter wavelength as TiO_2 content increases. The bands due to the interference color of the film appeared in the wavelength range of 350 to 800 nm. With increasing TiO_2 content, the amplitude of interference spectra increases due to the increase in refractive index of composite thin films.

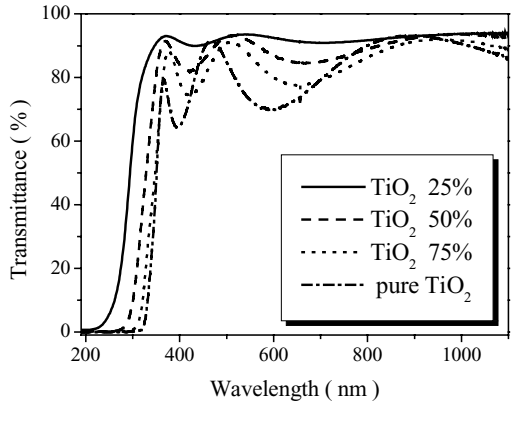

Figure 7 UV-VIS spectra of TiO_2-SiO_2 thin films calcined at 600°C.

The refractive index was calculated from the measured transmittance spectrum at a wavelength of 550 nm. The evaluation method used in this work is based on the analysis of the transmittance spectrum of a weakly absorbing film deposited on a non-absorbing substrate [24]. The refractive index $n(\lambda)$ over the spectral range is calculated by using the envelopes that are fitted to the measured extrema:

$$n(\lambda) = \sqrt{S + \sqrt{S^2 - n_0^2(\lambda) n_s^2(\lambda)}} \tag{2}$$

$$S = \frac{1}{2}\left(n_0^2(\lambda) + n_s^2(\lambda)\right) + 2n_0 n_s \frac{T_{max}(\lambda) - T_{min}(\lambda)}{T_{max}(\lambda) \times T_{min}(\lambda)} \tag{3}$$

where n_0 is the refractive index of air, n_s is the refractive index of the substrate, T_{max} is the maximum envelope, and T_{min} is the minimum envelope. The thickness of the films was adjusted to provide the best fits to the measured spectra. Deposited films are assumed to be homogeneous in the calculation. Fig. 8 shows the resultant refractive indices of the composite thin films calcined at various temperatures. We can see the refractive index increases from 1.50 to 2.23 with increasing TiO_2 content and calcination temperature. We cannot here calculate the refractive index of pure TiO_2 thin films calcined at 1000°C because of reduced transmittance. However, the refractive index would be considerably increased because the rutile phase has higher refractive index compared to the anatase phase. The increase in refractive index results from the increase in grain size and enhanced phase transformation with increasing TiO_2

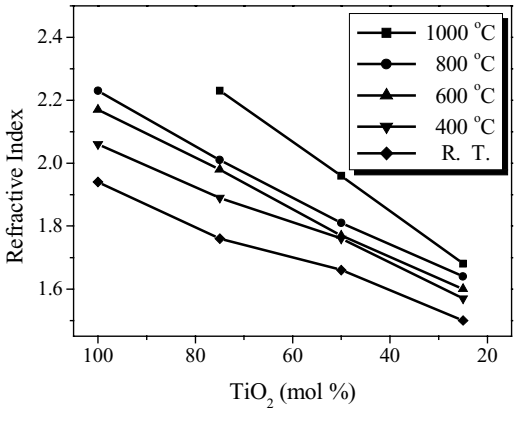

Figure 8 Refractive indices as a function of TiO_2 content in TiO_2-SiO_2 thin films calcined at various temperatures for 1 h. The refractive index is calculated from the measured transmittance spectrum at a wavelength of 550 nm.

content. From the Fig. 8, we can expect the change in the crystal phase of TiO_2 according to the change in refractive index.

In the Fig. 8, the refractive indices of $50TiO_2$-$50SiO_2$ thin films calcined at 400 and 600°C are almost identical. On the other hand, the refractive index of $75TiO_2$-$25SiO_2$ thin films calcined at 600°C is comparable to that calcined at 800°C. This result is expected from the XRD results. The $75TiO_2$-$25SiO_2$ films calcined at 600 and 800°C and $50TiO_2$-$50SiO_2$ film calcined at 800°C have anatase phase, while the $50TiO_2$-$50SiO_2$ film calcined at 400 and 600°C and $75TiO_2$-$25SiO_2$ film calcined at 400°C are amorphous. The crystallite size of the above anatase films is approximately 10 nm. SEM images in Figs 4 and 5 show the denser films are formed at a higher temperature. This result suggests that the refractive index of composite thin films depends largely on the film density, crystal structure and crystallite size of the films.

4. Conclusions

In this paper, we have fabricated TiO_2-SiO_2 composite films by sol-gel process and examined the dependence of their structural and optical properties on calcination temperature. We have found the physical properties of the composite thin films depend largely on TiO_2 content and calcination temperature. With increasing TiO_2 content, the intensity of Si—O bond peaks decreases and that of Ti—O bond peaks increases in the FTIR spectra. The amorphous-to-anatase transformation temperature is lowered as the TiO_2 content increases. The pure TiO_2 thin films calcined at 1000°C are a mixture of anatase and rutile phases. The increase in calcination temperature and TiO_2 content facilitates the TiO_2 crystallization in thin films. This is because SiO_2 hinders the formation of the anatase crystal of TiO_2. The rutile films are denser than the anatase films. The transmittance of the pure TiO_2 thin films calcined at 1000°C is significantly reduced at a shorter wavelength due to the increased absorption and scattering effect. The refractive index of thin films depends on the crystallite type, crystallite size, and density of the thin films. In the case of $50TiO_2$-$50SiO_2$, the refractive index of the thin films at 400°C is almost identical to that at 600°C. On the other hand, the refractive index of $75TiO_2$-$25SiO_2$ thin films at 600°C is close to that at 800°C. In this study, we successfully fabricated optical TiO_2-SiO_2 thin films with a refractive index ranging from 1.5 to about 2.2 by changing film composition and microstructure using a sol-gel dip coating method.

Acknowledgments

This work was supported by grant No. (R05-2001-000-00104-0) from the Basic Research Program of the Korea Science & Engineering Foundation. The authors thank Korea Basic Science Institute (Taegu Branch) for XRD and SEM measurements.

References

1. H. IMAI, H. HIRASHIMA and K. AWAZU, *Thin Solid Films* **351** (1999) 91.
2. D. R. UHLMANN, J. M. BOULTON, G. T. TEOWEE, L. WEISENBACH and B. J. ZELINSKI, *SPIE* **1328** (1990) 270.
3. J. D. MACKENZIE, *J. Ceram. Soc. Jpn.* **101** (1993) 1.
4. R. R. A. SYMS and A. S. HOLMES, *J. Non-Cryst. Solids.* **170** (1994) 223.
5. P. CHRYSICOPOULOU, D. DAVAZOGLOU, C. TRAPALIS and G. KORDAS, *Thin Solid Films* **323** (1998) 188.
6. H. KÖSTLIN, G. FRANK, G. HEBBINGHAUS, H. AUDING and K. DENISSEN, *J. Non-Cryst. Solids* **218** (1997) 347.
7. H. TANG, K. PRASAD, R. SANJINÉS and F. LÉVY, *Sens. Actuators* B **26/27** (1995) 71.
8. Y. YAN, S. R. CHAUDHURI and A. SARKAR, *J. Amer. Ceram. Soc.* **79** (1996) 1061.
9. J. ZHAI, T. YANG, L. ZHANG and X. YAO, *Ceram. Intern.* **25** (1999) 667.
10. J. YU, X. ZHAO and Q. ZHAO, *Mater. Chem. Phys.* **69** (2001) 25.
11. M. MENNIG, P. W. OLIVEIRA and H. SCHMIDT, *Thin Solid Films.* **351** (1999) 99.
12. C. J. BRINKER and M. S. HARRINGTON, *Sol. Energy Mater.* **5** (1981) 159.
13. H. YANAGI, T. HISHIKI, T. TOBITANI, A. OTOMO and S. MASHIKO, *Chem. Phys. Lett.* **292** (1998) 332.
14. S. McCULLOCH, G. STEWART, R. M. GUPPY and J. O. NORRIS, *Int J. Optelectron.* **9** (1994) 235.
15. G. W. DALE, H. H. FOX, B. J. J. ZELINSKI and L. WELLER-BROPHY, *Mater. Res. Soc. Better Ceram. Through Chem.* **IV** (1990) 371.
16. L. S. HSU, R. RUJKORAKARM, J. R. SITES and C. Y. SHE, *J. Appl. Phys.* **59** (1986) 3475.
17. E. J. KIM and S. H. HAHN, *Mater. Sci. Eng.* A **303** (2001) 24.
18. Z. LIU and R. DAVIS, *J. Phys. Chem.* **98** (1994) 1253.
19. A. MATSUDA, Y. MATSUNO and S. KATAYAMA, *J. Amer. Ceram. Soc.* **73** (1990) 2217.
20. B. D. CULLITY, "Elements of X-ray Diffraction" (Addison-Wesley Pub. Co., Notre Dam, 1978) p. 127.
21. D. MARDARE, M. TASCA, M. DELIBAS and G. I. RUSU, *Appl. Surf. Sci.* **156** (2000) 200.
22. E. J. KIM and S. H. HAHN, *Mater. Lett.* **49** (2002) 244.
23. T. HASHIMOTO, T. YOKO and S. SAKKA, *Bull. Chem. Soc. Jpn.* **67** (1994) 653.
24. J. C. MANIFACIER and J. GASIOT, *J. P. Fillard, J. Phys.* E **9** (1976) 1002.

Received 16 April 2003
and accepted 24 February 2004